

MAP fitting by count and inter-arrival moment matching

Walid W. Nasr, Ali Charanek & Bacel Maddah

To cite this article: Walid W. Nasr, Ali Charanek & Bacel Maddah (2018) MAP fitting by count and inter-arrival moment matching, *Stochastic Models*, 34:3, 292-321, DOI: 10.1080/15326349.2018.1474478

To link to this article: <https://doi.org/10.1080/15326349.2018.1474478>



Published online: 08 Oct 2018.



Submit your article to this journal [↗](#)



Article views: 139



View related articles [↗](#)



View Crossmark data [↗](#)



Citing articles: 3 View citing articles [↗](#)



MAP fitting by count and inter-arrival moment matching

Walid W. Nasr, Ali Charanek, and Bacel Maddah

Department of Industrial Engineering and Management, Faculty of Engineering and Architecture, American University of Beirut, Beirut, Lebanon

ABSTRACT

We identify key characteristics of a correlated point process which include moments of the time between arrivals as well as measures of variability and correlation obtained from the counting process over different time intervals. A computational framework to calculate these characteristics is presented for the general MAP(n). We present simple closed-form-expressions for the key characteristics and an efficient algorithm to fit a MAP(2) to a point process. The contributions of this article include 1) developing a computational framework, in the form of partial-moment differential equations (PMDEs) and linear equations to derive a compact matrix exponential expression for the count process moments of a MAP(n), 2) developing an efficient and accurate algorithm to fit a MAP(2) based on count and inter-arrival moments.

ARTICLE HISTORY

Received 9 December 2015
Accepted 6 May 2018

KEYWORDS

Correlated process; count process; distribution fitting; Markovian arrival process; point process

1. Introduction

The Markovian arrival process (MAP), as presented by Neuts,^[31] and the special case of the Markovian modulated Poisson process (MMPP),^[11] are stochastic processes that have the flexibility to capture inter-arrival dependence and have received attention due to their applicability in several fields. The MAP notation commonly used in the recent literature and in this work is based on the notation of Lucantoni et al.^[24] The majority of the literature on fitting point processes via a Markovian process matches the first two or three inter-arrival moments and the lag- k inter-arrival auto-correlation for $k=1$ or $k>1$ (e.g. Bodrog et al.,^[5] Diamond and Alfa^[10] and Horvath et al.^[16]). Fitting moments of the count process to capture inter-arrival variability and correlation is addressed in Whitt^[41] and Gusella.^[12] The index of dispersion of counts (IDC) is utilized as a measure of variability in the count process in Gusella,^[12] Sriram and Whitt,^[39] Heffes and Lucantoni,^[15] and Nasr and Taaffe^[28] among others. Indexes of dispersion

for inter-arrivals and counts have long been used in the analysis of point.^[9] Notice that Gusella^[12] and Whitt^[41] use count moments to fit MMPP and Ph, phase-type (hyper-exponential and Erlang) which are special cases of the MAP, to non-renewal processes. The work in Feldmann and Whitt^[13] examines the flexibility of the hyper-exponential distribution in fitting the inter-arrival time where they show that every distribution with a completely monotone probability distribution function can be accurately fitted by an $n \geq 1$ phase hyper-exponential distribution. Fitting approaches which are a hybrid combination of inter-arrival moments and the count process limit characteristics are considered in Whitt^[41] and Albin^[1] and with applications in Whitt.^[42]

In this article, we explore fitting inter-arrival moments as well as moments of the count process. The characteristics of the count process considered in this article include the behavior of the IDC over short and long time intervals. We define a property of the count process which measures the asymptotic variance of the count process relative to that of a renewal process with the same first two inter-arrival moments. We refer to the measure as the coefficient of variation in the count process due to correlation (CVC). The CVC is equal to zero for a renewal process and approaches 1 or -1 for highly correlated processes.

A fitting approach which only matches inter-arrival moments does not capture dependence, but would provide an accurate fit if the approximated process is a renewal point process. Accounting for the moments of the count process would result in more accurate approximations for correlated point processes. This provides the intuition behind the fitting approach presented in this article which minimizes a weighted sum based on the CVC as follows. The fitting approach utilizes the CVC as a relative weight for the IDC values relative to the inter-arrival moments. Although the minimal representation of a MAP(2) is four parameters, the fitting algorithm fits a weighted combination of more than four characteristics where the weights depend on the impact of the correlation on the point process as measured by the CVC. Higher weights are assigned to the inter-arrival moments for values of CVC which are close to 0. Similarly, higher weights are assigned to the count moment measures as the CVC approaches 1 or -1 .

It is well established in the literature on queuing theory that ignoring third moments and only accounting for second order descriptors can lead to inaccurate approximations, Sahin and Perrakis,^[36] Whitt,^[43] Johnson and Luhman^[19] and Begin and Brandwajn,^[4] among others. The work in Andersen et al.^[2] illustrates that second-order descriptors of the counting and the inter-arrival processes (although commonly used standard descriptors) are not sufficient descriptors by themselves. This is illustrated by

considering the time reversal of a MAP which is shown to have the same descriptors for the counting and inter-arrival process, but each process results in different queuing system measures. Only in special cases would it be possible to match the entire set of chosen key characteristics of a point process. Accordingly, the term “fitting” would not in general imply perfect correspondence between the approximated point process and the “fitted” point process. Instead, most of the work targets a chosen set of key characteristics of the point process. In [Section 1.1](#) we review the existing approaches to calculate the count moments of a MAP(n) and in [Section 1.2](#) we consider the literature which examines the characteristics and limitations of a two-source MAP.

1.1. Approaches to calculate the count moments of a MAP(n)

The moment matrices as defined by Neuts^[31] and Narayana and Neuts^[25] denote the partial moments of the count process over a time interval $[0, t]$ and the state of the MAP at time t conditioned on the state of the MAP at time 0. The work in Neuts^[31] presents a numerical approach to compute the first two moment-matrices (mean matrix and second-moment matrix). The computation of the first two moment matrices of the count process is further investigated in Narayana and Neuts^[25] for the more general Batch-MAP (BMAP) case. Numerical approaches to calculate the k th moment matrices for $k > 2$ are computationally extensive and are not presented in Narayana and Neuts.^[25] The work in Neuts and Li^[32] presents numerical approaches to calculate the probability distribution of the counting process over a time interval t . Obtaining the moment matrices directly from the probability distribution of the counting process can be computationally extensive since over a time interval of duration t , the state space of the number of counts is infinite. Consequently, an upper limit on the number of counts has to be considered. The authors in Buchholz et al.^[7] point out that the first moment of the count process is easy to compute, unlike higher order moments.

The work in Nielsen et al.^[30] presents a homogeneous set of differential equations to solve for the k th moment matrices of MAP of n . In this work, we explicitly present the solution of the differential equations of Nielsen et al.,^[30] which calculate moment matrices, by a compact matrix exponential expression. Accordingly, the computational efficiency of solving for k th moment matrix of a MAP of order n is dependent on the dimensions of the corresponding matrix exponential, $(k + 1) n \times (k + 1) n$. For the purpose of this work, we consider relatively small problems where $k \leq 2$ and $n \leq 4$, and the matrix exponential is a convenient approach which is readily available in several mathematical software. This is further motivated by

the attention MAPs of modest to low order are receiving in the literature. The work in Kriege and Buchholz^[22] conduct an empirical comparison of different methods to fit a MAP to three different real traces where the fitting approaches used MAPs of order 2 to 6. The work in Okamura et al.^[33] considers parameter estimation of MAPs with order 2, 3 and 6. The authors in Kriege and Buchholz^[23] utilize a MAP of order 5 to fit internet traffic. Recently, the work in Zheng et al.^[45] estimate MAP parameters based on data for arrival streams collected from a web server where the fitted MAP was of order 2. Similarly, in the context of computer systems and network performance, MAPs of order 2 are utilized to fit real data representing server caching request epochs.^[14] In the context of supply chain systems, the recent work in Sivakumar and Arivarignan,^[37] Nasr and Maddah^[27] and Nasr and Elshar,^[26] among others, assume the demand process follows a Markovian Process where the numerical investigations account for MAPs of orders 2, 3 and 4.

In the case where higher moments and higher order MAPs are required, an alternative is the uniformization approach presented in Narayana and Neuts^[25] for the calculating the second-moment matrices. This also applies to the more recent extension in Nielsen et al.^[30] to compute the k th moment matrices. The computational approach of Narayana and Neuts^[25] and Nielsen et al.^[30] is based on solving integrals of matrix exponentials which can be traced back to Van Loan.^[44]

1.2. Characteristics of MAP(2)

We review the relevant literature which identifies the characteristics which define a MAP(2) as well as describes a range on these characteristics. The work in Andersen and Nielsen^[3] investigates the limitation of a MAP(2) and shows that the rate, IDC, and the index of dispersion for intervals (IDI) completely determines the MAP(2) process. The authors also indicate the significance of identifying the limitation of the MAP(2) in order to squeeze the maximum information at hand into the fitted process. The work in Telek and Hovarth^[40] on the minimal representation of MAPs illustrates that the minimal representation of a MAP(2) is four characteristics where for example a MAP(2) is fully defined by the first three inter-arrival moments and the lag correlation. The work in Bodrog et al.^[5] further examines the limitation of the two-source MAP where they consider the feasible space characterized by four characteristics (the first three inter-arrival moments and lag correlation). In the case where the selected characteristics of a point process fall outside the feasible space, then the authors define a Euclidean distance as a measure of the fitting accuracy provided by a two-state MAP. In the case where the Euclidean distance is zero, a

two-state MAP provides an exact fit to the selected characteristics. The recent work in Kim^[20] also considers the moments of the MAP(2) as a function of the four-parameter canonical representation and investigates the feasible range on the parameters. The work in Heindl et al.^[18] also investigates the limitations of a MAP(2) and derives bounds on the correlation parameters. The authors demonstrate the applicability of the findings on the decomposition of queuing networks. The convergence of the autocorrelation pattern of a MAP(2) is investigated in Ramirez-Cobo and Carrizosa^[34] and the authors argue for the inadequacy of a MAP(2) process to model seasonal data. The work in Rodriguez et al.^[35] explores the correlation patterns for a two state MAP as well as the influence of the inter-arrival correlation on the counting process.

The remainder of this article is organized as follows. The MAP(n) notation and characteristics are presented in Section 2. Closed-form expressions of the count process characteristics and the first three inter-arrival moments are presented in Sections 3.1 and 3.2 respectively for the MAP(2) case. The fitting algorithm is presented in Section 4. In Section 5, we use the algorithm presented in Section 4 to fit a MAP(2) to point processes, and we numerically compare our fitting method to existing algorithms in the literature. Finally, Section 6 concludes the article, and presents ideas for future research.

2. MAP(n) notation and characteristics

In this section, we present the notation for the MAP(n) and a computational framework for estimating its key characteristics. The MAP(n) notation is presented in Section 2.1. Partial-moment differential equations (PMDEs) to estimate the moments of MAP(n) counts are developed in Section 2.2. Related measures of count variability and correlation, including the new CVC measure, are given in Section 2.3. Finally, linear equations to estimate the inter-arrival time moments are presented in Section 2.4.

2.1. Notation – MAP(n)

A MAP(n) is commonly defined by an n phase continuous time Markov chain (CTMC) where the non-diagonal entries of the $(n \times n)$ matrix, \mathbf{D}_0 , contain the transition rates within the CTMC that result in no arrivals. The $(n \times n)$ matrix, \mathbf{D}_1 , contains the transition rates within the CTMC that result in an arrival. We refer to Lucantoni et al.^[24] and Telek and Horvath^[40] for further information on the MAP(n) representation. Let $\lambda_{i,j} = \mathbf{D}_1(i,j)$ for $i, j = 1, \dots, n$, and $\alpha_{i,j} = \mathbf{D}_0(i,j)$ for $i, j = 1, \dots, n$ and $i \neq j$. The diagonal entries of \mathbf{D}_0 are $\mathbf{D}_0(i,i) = -\sigma_i$ for $i = 1, \dots, n$ where $\sigma_i = \sum_{j=1, j \neq i}^n \alpha_{i,j} + \sum_{j=1}^n \lambda_{i,j}$.

2.2. Moments of the MAP(n) count process

Consider a MAP(n) with parameters defined in Section 2.1. and let $C_t(\tau)$ represent the resulting count process, i.e. number of arrivals, over the time interval $[t, t + \tau)$. Also, let $A(t)$ be the state of the embedded CTMC at time t ; i.e., $A(t) = i$ if the MAP(n) is in Phase i at time t , $i = 1, 2, \dots, n$. At time $(t + \tau)$, we define a joint phase-and-count state by the count during time interval $[t, t + \tau)$, $C_t(\tau)$, and the state of the MAP(n), $A(t + \tau)$. Let $P_{\ell,c,t}(\tau) = P(A(t + \tau) = \ell, C_t(\tau) = c)$ be the probability of being in state (ℓ, c) for $\ell = 1, 2, \dots, n$ and $c = 1, 2, \dots$. The Kolmogorov forward differential equations (KFEs) for $P_{\ell,c,t}(\tau)$ are given in Equation (1). Let $P'_{\ell,c,t}(\tau) = \frac{\partial P_{\ell,c,t}(\tau)}{\partial \tau}$ and denote $P_{\ell,c,t}(\tau)$ and $P'_{\ell,c,t}(\tau)$ by $P_{\ell,c}$ and $P'_{\ell,c}$, respectively, to simplify the presentation.

$$P'_{\ell,c} = -\sigma_\ell P_{\ell,c} + \sum_{i=1, i \neq \ell}^n \alpha_{i,\ell} P_{i,c} + \sum_{i=1}^n \lambda_{i,\ell} P_{i,c-1}. \quad (1)$$

The set of KFEs presented in Equation (1) is an infinite set of differential equations since there is no upper limit on the count within a time interval. In this article, we utilize the KFEs to derive a finite set of PMDEs to solve for the moments of $C_t(\tau)$. This is based on the fact the PMDE of the k th moment of the count process $C_t(\tau)$ is given by,

$$E \left[C_t^k(\tau) \mathbf{I}(A(t + \tau) = \ell) \right] = \sum_{c=1}^{\infty} c^k P_{\ell,c}, \quad \text{for } \ell = 1, \dots, n. \quad (2)$$

where the indicator function $\mathbf{I}(\cdot)$ is 1 if the expression in 1 is true and 0 otherwise. Let

$$E \left[C_t^k(\tau), A(t + \tau) = \ell \right] = E \left[C_t^k(\tau) \mathbf{I}(A(t + \tau) = \ell) \right],$$

i.e., $E[C_t^k(\tau), A(t + \tau) = \ell] = E[C_t^k(\tau) | A(t + \tau) = \ell] \text{Prob}(A(t + \tau) = \ell)$.

The finite set of PMDEs to solve for the k th moment of $C_t(\tau)$ is presented below in Equation (3) and expanded in Equation (4). The derivative is with respect to τ .

$$\begin{aligned} E' \left[C_t^k(\tau), A(t + \tau) = \ell \right] &= E' \left[C_t^k(\tau) \mathbf{I}(A(t + \tau) = \ell) \right] \\ &= \sum_{c=1}^{\infty} c^k P'_{\ell,c}, \quad \text{for } \ell = 1, \dots, n. \end{aligned} \quad (3)$$

The PMDEs of the k th moment of the count process $C_t(\tau)$ are,

$$E' \left[C_t^k(\tau), A(t + \tau) = \ell \right] = -\sigma_\ell E \left[C_t^k(\tau), A(t + \tau) = \ell \right]$$

$$\begin{aligned}
 & + \sum_{\substack{i=1 \\ i \neq \ell}}^n \alpha_{i,\ell} E \left[C_t^k(\tau), A(t + \tau) = i \right] \\
 & + \sum_{i=1}^n \lambda_{i,\ell} \left(\sum_{j=1}^k \binom{k}{j} E \left[C_t^j(\tau), A(t + \tau) = i \right] \right. \\
 & \left. + P(A(t + \tau) = i) \right), \tag{4}
 \end{aligned}$$

for $\ell = 1, \dots, n$ and $k = 1, 2, 3, \dots$. We refer to Nielsen et al.^[30] for a compact matrix representation of the differential equations in 4. Notice that solving for $C_t^k(\tau)$ using Equation (4) requires solving the first $k-1$. Solving for the second moment PMDEs requires solving the zeroth and first PMDEs. The detailed derivation of Equation (4) is given in Appendix 1. The zeroth PMDEs are obtained from Equation (3) for $k=0$,

$$\begin{aligned}
 P'(A(t + \tau) = \ell) & = \sum_{c=1}^{\infty} P'_{\ell,c} \\
 & = -\sigma_{\ell} P(A(t + \tau) = \ell) + \sum_{i=1, i \neq \ell}^n \alpha_{i,\ell} P(A(t + \tau) = i) \\
 & \quad + \sum_{i=1}^n \lambda_{i,\ell} P(A(t + \tau) = i), \text{ for } \ell = 1, \dots, n, \tag{5}
 \end{aligned}$$

A matrix representation for the homogenous probability differential equations in Equation (5) is presented below,

$$\underset{(n \times 1)}{\mathbf{\Pi}'_{t+\tau}} = \underset{(n \times n)}{\mathbf{Q}_0} \underset{(n \times 1)}{\mathbf{\Pi}_{t+\tau}}, \tag{6}$$

where $\mathbf{\Pi}_{t+\tau}(\ell) = P(A(t + \tau) = \ell)$ for $\ell = 1, \dots, n$, and $\mathbf{Q}_0 = (\mathbf{D}_0 + \mathbf{D}_1)^T$. A matrix exponential solution to the homogenous probability differential equations in Equations (5) and (6),

$$\mathbf{\Pi}_{t+\tau} = (\mathbf{e}^{\mathbf{Q}_0 \tau}) \mathbf{\Pi}_t. \tag{7}$$

Solving for the first moment PMDEs requires solving Equation (4) (for $k=1$) and 5 concurrently, and can be calculated by solving the following matrix exponential,

$$\mathbf{F}_t(\tau) = (\mathbf{e}^{\mathbf{Q}_1 \tau}) \mathbf{F}_t(0), \tag{8}$$

$$\underset{(2n \times 2n)}{\mathbf{Q}_1} = \left(\begin{array}{c|c} \underset{(n \times n)}{\mathbf{Q}_0} & \underset{(n \times n)}{\mathbf{0}} \\ \hline \underset{(n \times n)}{\mathbf{D}_1^T} & \underset{(n \times n)}{\mathbf{Q}_0} \end{array} \right). \tag{9}$$

The vector $\mathbf{F}_t(\tau)$ is $2n \times 1$ where the first n entries correspond to the probabilities in $\mathbf{\Pi}_{t+\tau}$ and the entries $n + 1$ to $2n$ represent the first partial-moments $E[C_t(\tau), A(t + \tau) = \ell]$ for $\ell = 1, \dots, n$. Similarly, solving for the second PMDEs, $k = 2$ in Equation (4), also requires solving for the first PMDEs,

$$\mathbf{S}_t(\tau) = (\mathbf{e}^{\mathbf{Q}_2\tau}) \mathbf{S}_t(0), \tag{10}$$

$$\mathbf{Q}_2 = \begin{pmatrix} \mathbf{Q}_1 & & \mathbf{0} \\ \hline (2n \times 2n) & & (2n \times n) \\ \mathbf{D}_1^T & 2 \mathbf{D}_1^T & \mathbf{Q}_0 \\ \hline (n \times n) & (n \times n) & (n \times n) \end{pmatrix}. \tag{11}$$

The vector $\mathbf{S}_t(\tau)$ is $3n \times 1$ where the first $2n$ entries correspond to $\mathbf{F}_t(\tau)$ and the entries $2n + 1$ to $3n$ represent the second partial-moments $E[C_t^2(\tau), A(t + \tau) = \ell]$ for $\ell = 1, \dots, n$. In general, solving for the k th partial-moments of the count process over the time interval $[t, t + \tau]$ as well as the j th partial-moments for $j = 0, \dots, k - 1$,

$$C^{(k)}_t(\tau) = (\mathbf{e}^{\mathbf{Q}_k\tau}) C^{(k)}_t(0), \tag{12}$$

$$\mathbf{Q}_k = \begin{pmatrix} & & & & \mathbf{Q}_{k-1} & & \mathbf{0} \\ & & & & \hline & & & & (kn \times kn) & & (kn \times n) \\ \mathbf{D}_1^T & \binom{k}{1} \mathbf{D}_1^T & \dots & \binom{k}{i} \mathbf{D}_1^T & \dots & \binom{k}{k-1} \mathbf{D}_1^T & \mathbf{Q}_0 \\ \hline (n \times n) & (n \times n) & & (n \times n) & & (n \times n) & (n \times n) \end{pmatrix}. \tag{13}$$

The vector $C^{(k)}_t(\tau)$ is $(k + 1)n \times 1$ where the first $(k n)$ entries correspond to $C^{(k-1)}_t(\tau)$ and the entries $(k n + 1)$ to $(k + 1)n$ represent the k th partial-moments $E[C_t^k(\tau), A(t + \tau) = \ell]$ for $\ell = 1, \dots, n$. The computational efficiency of solving the matrix \mathbf{Q}_k is dependent on the dimensions $(k + 1) n \times (k + 1) n$.

2.3. Measures of variability and correlation in the count process

Here and throughout this work, $C(\tau)$ is the stationary count process over an interval of length τ ; i.e. $C(\tau) = \lim_{t \rightarrow \infty} C_t(\tau)$. The index of dispersion for count (IDC) over a time interval of length τ is given by

$$IDC(\tau) = \frac{\text{Var}[C(\tau)]}{E[C(\tau)]}. \tag{14}$$

We refer the reader to Gusella^[12] for more details on $IDC(\tau)$. Fitting the IDC or the second moment of a count process captures the correlation between consecutive points, see Gusella^[12] and Whitt.^[41] Variability in the count process of a point process can be due to the variability of the inter-arrivals as well as the dependence between inter-arrivals. Here we introduce a measure which is the coefficient of variability in the count process due to correlation (CVC). For a count process $C(\tau)$ with inter-arrival first two moments m_1 and m_2 , let $C_R(\tau)$ be the corresponding count of a renewal process with the same inter-arrival first two moments m_1 and m_2 . Notice that for the case where the count process $C(\tau)$ is generated from a MAP, then the embedded Phase-type process can serve as the corresponding $C_R(\tau)$ count process.

In the case where the variability of $C(\tau)$ exceeds that of $C_R(\tau)$ as $\tau \rightarrow \infty$, $\lim_{\tau \rightarrow \infty} IDC[C(\tau)] \geq \lim_{\tau \rightarrow \infty} IDC[C_R(\tau)]$, we define the CVC of a point process,

$$CVC = 1 - \lim_{\tau \rightarrow \infty} \frac{IDC[C_R(\tau)]}{IDC[C(\tau)]} = 1 - \lim_{\tau \rightarrow \infty} \frac{Var[C_R(\tau)]}{Var[C(\tau)]}, \tag{15}$$

In the case where the variability of the correlated count process, $C(\tau)$, is less than the corresponding renewal process, $C_R(\tau)$, $\lim_{\tau \rightarrow \infty} IDC[C(\tau)] < \lim_{\tau \rightarrow \infty} IDC[C_R(\tau)]$,

$$CVC = \lim_{\tau \rightarrow \infty} \frac{IDC[C(\tau)]}{IDC[C_R(\tau)]} - 1 = \lim_{\tau \rightarrow \infty} \frac{Var[C(\tau)]}{Var[C_R(\tau)]} - 1. \tag{16}$$

Combining Equations (15) and (16),

$$CVC = \lim_{\tau \rightarrow \infty} \frac{Var[C(\tau)] - Var[C_R(\tau)]}{\max(Var[C_R(\tau)], Var[C(\tau)])}, \tag{17}$$

The variance of the renewal process can be expressed as (see Smith^[38] and Whitt^[41]),

$$Var[C_R(\tau)] = m_1^{-3}(m_2 - m_1^2)\tau + m_1^{-4}((5/4)m_2^2 - (2/3)m_3 - m_1 - (1/2)m_2 - m_1^2) + o(1), \tag{18}$$

where m_k is the k th moment of the inter-arrival process for $k = 1, 2, \dots$. The value of the CVC as expressed in Equation (17) is 0 for a renewal process. For the case where $Var[C(\tau)] \gg Var[C_R(\tau)]$, the CVC approaches 1 which can be clearly seen from Equation (15). Similarly, the CVC approaches -1 when $Var[C(\tau)] \ll Var[C_R(\tau)]$. This results in a range of $-1 < CVC < 1$. Correlation within a point process can result in a reduction in the variability in the count process and is indicated by a negative CVC. As an illustrative example on a case where the CVC approaches -1, consider a point process (see example in Whitt^[41]) where the i th inter-arrival time is X_i and let

$P\{(X_i, X_{i+1}) = (1, 2) \text{ or } (2, 1)\} = 1$ for all i and $P(X_1 = 1) = P(X_1 = 2) = 1/2$. The inter-arrival moments are calculated as $m_k = (0.5)(1^k) + (0.5)(2^k)$. The first three inter-arrival moments are $m_1 = 1.5, m_2 = 2.5$ and $m_3 = 4.5$. The limit of the IDC for a renewal process with the same first three inter-arrival moments results in $\lim_{\tau \rightarrow \infty} \text{IDC}[C_R(\tau)] = 0.111 > 0$. The CVC $\rightarrow -1$, since $\lim_{\tau \rightarrow \infty} \text{IDC}[C(\tau)] \rightarrow 0$. In the numerical examples section we present MAP(3) and MAP(4) cases where the CVC is varied to take on negative and positive values. We utilize the CVC in our MAP(2) fitting algorithm in [Section 4](#) to assign weights to correlation-related characteristics as well as inter-arrival characteristics. The weights are assigned such that they are increasing for the characteristics that capture correlation as CVC approaches -1 and 1 , and decreasing as the CVC approaches 0 . Similarly, the weights for the inter-arrival moments are increasing as the CVC approaches 0 .

2.4. MAP(n) stationary inter-arrival moments

Let m_k be the k th moment of the inter-arrival process for $k = 1, 2, \dots$. Let ξ_i be the stationary probability that an arbitrary arrival epoch begins in Phase i for $i = 1, \dots, n$ and let ξ be the corresponding $n \times 1$ vector. The steady-state probabilities ξ can be calculated by solving the following system of linear equations,

$$\xi^T (-\mathbf{D}_0)^{-1} \mathbf{D}_1 = \xi^T, \quad \text{and} \quad \xi^T \mathbf{e} = 1, \quad (19)$$

where \mathbf{e} is an $n \times 1$ vector of 1 s. The k th moment can be calculated as,

$$m_k = k! \xi^T (-\mathbf{D}_0)^{-k} \mathbf{e} \quad \text{for } k = 1, 2, \dots \quad (20)$$

We refer the reader to Bodrog et al.^[5] or Nelson and Gerhardt^[29] for further information on computing the inter-arrival moments. In [Section 3.2](#), we present closed-form expressions to calculate the first three inter-arrival moments for the MAP(2) special case.

3. The MAP(2) process

In this section, we present closed-form expressions for the count and inter-arrival characteristics, as presented in [Section 2](#), for the MAP(2) special case. In [Section 3.1](#) we consider the PMDEs of [Section 2.2](#) for the MAP(2) special case and present closed-form expressions for the IDC and CVC characteristics. Closed-form expressions for the first three inter-arrival moments of a MAP(2) are presented in [Section 3.2](#). Following the notation of [Section 2.1](#), the MAP(2) special case is defined by the six parameters which are the non diagonal entries of \mathbf{D}_0 and the entries of \mathbf{D}_1 . Denote the MAP(2) parameters by $\mathbf{x} = (\alpha_{12}, \alpha_{21}, \lambda_{11}, \lambda_{12}, \lambda_{21}, \lambda_{22})$. A six parameter notation is redundant, but is utilized in the equations presented in this

section since the standard MAP notation based on \mathbf{D}_0 and \mathbf{D}_1 is the more intuitive and commonly used notation in the literature. Since fitting over six parameters is not a numerically efficient approach, we express the MAP(2) in terms of a four parameter canonical representation as presented in Bodrog et al.^[6] in the fitting algorithm of Section 4.2.

3.1. The MAP(2) count process

The following theorem presented closed-form expressions for count moments.

Theorem 1. *The first two moments of count of a MAP(2) over an interval of length τ are*

$$E[C(\tau); \mathbf{x}] = \frac{\tau}{m_1} = \frac{\theta_2 \tau}{\beta}, \tag{21}$$

$$E[C^2(\tau); \mathbf{x}] = \frac{\theta_1}{\beta^2} \tau + \frac{\theta_2^2}{\beta^2} \tau^2 - \frac{\theta_1}{\beta^3} (1 - e^{-\beta\tau}), \tag{22}$$

where $\theta_1 = 2(c_4 - c_3) (c_2 c_6 - c_1 c_5) + (c_5 + c_6) \beta^2$, $\theta_2 = (c_2 c_3 + c_1 c_4)$, $\beta = c_1 + c_2$, $c_1 = \lambda_{12} + \alpha_{12}$, $c_2 = \lambda_{21} + \alpha_{21}$, $c_3 = \lambda_{11} + \lambda_{12}$, $c_4 = \lambda_{22} + \lambda_{21}$, $c_5 = \sigma_1 P_1 - \alpha_{21} P_2$, $c_6 = \sigma_2 P_2 - \alpha_{12} P_1$, and P_i is the stationary probability of being in Phase i ,

$$P_1 = \frac{c_2}{c_1 + c_2} \text{ and } P_2 = \frac{c_1}{c_1 + c_2}. \tag{23}$$

Proof. See Appendix 3. □

Notice that fitting the first moment of the inter-arrival process, m_1 , is equivalent to fitting the first moment count process, $E[C(\tau)]$ (Equation (21)). A more computationally extensive alternative to calculate the count moments presented in Theorem 1 is to numerically integrate the corresponding differential equations (Equations (40–42)). The following theorem also presents closed-forms for the MAP(2) IDC as well as the asymptotic case where $\tau \rightarrow \infty$.

Theorem 2. *The IDC for a MAP(2) is*

$$IDC(\tau; \mathbf{x}) = \frac{\frac{\theta_1}{\beta} \tau - \frac{\theta_1}{\beta^2} (1 - e^{-\beta\tau})}{\theta_2 \tau}. \tag{24}$$

where θ_1 , θ_2 and β are given in Theorem 1. As $\tau \rightarrow \infty$,

$$\text{IDC}(\infty; \mathbf{x}) = \lim_{\tau \rightarrow \infty} \text{IDC}(\tau; \mathbf{x}) = \frac{\theta_1}{\beta\theta_2}. \tag{25}$$

Proof. See Appendix 3. □

Finally, for the CVC characteristic defined in Section 2.3, we also present a closed-form expression.

Corollary 1. The CVC of a MAP(2),

$$\text{CVC}(\mathbf{x}) = \frac{\theta_1 \beta^{-2} - (m_2 - m_1^{-2}) m_1^{-3}}{\max(\theta_1 \beta_2^{-2}, (m_2 - m_1^2) m_1^{-3})} \tag{26}$$

where m_1 and m_2 are the first two moments of the stationary inter-arrival time, which are given in Equation (27) below, θ_1 and β are given in Theorem 1.

Proof. Proof follows from Equation 17. □

3.2. MAP(2) stationary inter-arrival moments

The first three MAP(2) inter-arrival moments can be calculated by first solving the system of linear equations in Equation (19), then solving Equation (20) for $k=1, 2$ and 3 . In this section, we also present closed-form expressions to calculate the first three inter-arrival moments that exploit the parameters c_1, c_2, c_3 and c_4 (presented in Section 3.1). The closed form inter-arrival characteristics are presented for completion and would result in an efficient approach to calculate the count characteristics and inter-arrival moments concurrently. The first three moments of the inter-arrival time of a MAP(2) can be expressed as,

$$\begin{aligned} m_1(\mathbf{x}) &= \frac{\beta}{\theta_2}, & m_2(\mathbf{x}) &= \frac{2 (\sigma_1 + \alpha_{21}) c_1 + 2 (\sigma_2 + \alpha_{12}) c_2}{(\sigma_1 \sigma_2 - \alpha_{12} \alpha_{21}) \theta_2}, \\ m_3(\mathbf{x}) &= \frac{6 [\sigma_1^2 + \alpha_{21} \sigma_2 + \alpha_{21} (\sigma_1 + \alpha_{12})] c_1 + 6 [\sigma_2^2 + \alpha_{12} \sigma_1 + \alpha_{12} (\sigma_2 + \alpha_{21})] c_2}{(\sigma_1 \sigma_2 - \alpha_{12} \alpha_{21})^2 \theta_2}, \end{aligned} \tag{27}$$

where $\beta, \theta_2, c_1,$ and c_2 are given in Theorem 1. In the next section, we present an algorithm to fit a MAP(2) to the count and inter-arrival key characteristics.

4. Counts and inter-arrival (moment) matching (CIM) algorithm

In Section 3, we presented closed-form expressions for the key characteristics of a MAP(2). In this section, we present an algorithm that fits a

MAP(2) to a point process by matching these characteristics. The key characteristics of the point process include the first three moments of the inter-arrival process as well as the IDC of the count process over intervals of different lengths. An estimate of the CVC metric of the point process, defined in Section 2.3, is also used to assign weights for the count-related characteristics in our fitting algorithm. We refer to our fitting algorithm by the Counts and Inter-arrival (Moment) Matching (CIM) algorithm.

4.1. Computing the key characteristics

The CIM fits five characteristics where the first three are the inter-arrival moments of the approximated/source process, \widetilde{m}_i for $i=1, 2$ and 3 . The fourth and fifth characteristics capture variability of the count process over short and long time intervals, respectively. Denote $\widetilde{\text{IDC}}(\tau)$ as the IDC of the source count process over a time interval of length τ . The variability of the count process is captured by fitting the transient shape of the IDC curve over k selected times $\tau_{s,j}$ for $j=1, \dots, k$. The measure used for long-term variability is $\widetilde{\text{IDC}}(\tau_\ell)$ where τ_ℓ is large enough such that $|\widetilde{\text{IDC}}(t) - \widetilde{\text{IDC}}(\tau_\ell)| / \widetilde{\text{IDC}}(\tau_\ell) < \epsilon$ for every $t > \tau_\ell$ and for a given $\epsilon > 0$. In the numerical examples section we choose τ_ℓ to be large enough to satisfy $\epsilon < 0.001$.

Capturing the behavior of the count process over short intervals is achieved by minimizing the squared errors between the transient shape of the source IDC curve and the approximating IDC at the k selected points at times $\tau_{s,j}$ for $j=1, \dots, k$. The transient shape of the $\widetilde{\text{IDC}}$ curve is captured by solving for the values of $\tau_{s,j}$ which satisfy,

$$\widetilde{\text{IDC}}(\tau_{s,j}) = \widetilde{\text{IDC}}_{\min} + \frac{j}{k+1} \left(\widetilde{\text{IDC}}_{\max} - \widetilde{\text{IDC}}_{\min} \right), \text{ for } j = 1, \dots, k, \quad (28)$$

where $\widetilde{\text{IDC}}_{\min}$ and $\widetilde{\text{IDC}}_{\max}$ are the minimum and maximum values of the IDC respectively. Let $\kappa = t/m_1$ and $\kappa_i = \tau_{s,j}/m_1$ for $i=1, \dots, k$. Two examples to illustrate the selection of $\tau_{s,j} = \kappa_j m_1$, utilizing Equation (28) are presented in Appendix 4.

4.2. The algorithm

The CIM algorithm calculates the MAP(2) parameters represented by the vector $\mathbf{x} = (\alpha_{12}, \alpha_{21}, \lambda_{11}, \lambda_{12}, \lambda_{21}, \lambda_{22})$ that results in the best fit by minimizing a sum of weighted square errors (SSE),

$$\Phi(\mathbf{x}) = \sum_{i=1}^5 w_i \Upsilon_i(\mathbf{x}), \quad (29)$$

where

$$\Upsilon_i(\mathbf{x}) = \left(\frac{m_i(\mathbf{x}) - \tilde{m}_i}{\tilde{m}_i} \right)^2, \text{ for } i = 1, 2, 3 \quad (30)$$

$$\Upsilon_4(\mathbf{x}) = \frac{1}{k} \sum_{j=1}^k \left(\frac{\text{IDC}(\tau_{s,j}; \mathbf{x}) - \widetilde{\text{IDC}}(\tau_{s,j})}{\widetilde{\text{IDC}}(\tau_{s,j})} \right)^2, \quad (31)$$

$$\Upsilon_5(\mathbf{x}) = \left(\frac{\text{IDC}(\tau_\ell; \mathbf{x}) - \widetilde{\text{IDC}}(\tau_\ell)}{\widetilde{\text{IDC}}(\tau_\ell)} \right)^2, \quad (32)$$

and $m_i(\mathbf{x})$, for $i = 1, 2$ and 3 , are given in Equation (27). The $\text{IDC}(\tau; \mathbf{x})$ is given in Theorem 2, and w_i are the corresponding weights for $i = 1, \dots, 5$.

A transformation between \mathbf{x} and the canonical representation results in $\mathbf{x}^c = (\tilde{\lambda}_1, \tilde{\lambda}_2, \tilde{a}, \tilde{b})$ where,

$$\alpha_{12} = \tilde{\lambda}_1(1 - \tilde{a}), \quad \alpha_{21} = 0, \quad \lambda_{11} = I_{\tilde{b}} \tilde{\lambda}_1 \tilde{a}, \quad \lambda_{22} = (1 - I_{\tilde{b}} + \tilde{b}) \tilde{\lambda}_2,$$

$$\lambda_{12} = \tilde{\lambda}_1 - \lambda_{11} - \alpha_{12}, \quad \lambda_{21} = \tilde{\lambda}_2 - \lambda_{22}, \quad (33)$$

and the indicator function $I_{\tilde{b}} = 1$ if $\tilde{b} \geq 0$, and $I_{\tilde{b}} = 0$ otherwise. Additionally, $0 < \tilde{\lambda}_1 \leq \tilde{\lambda}_2, 0 \leq \tilde{a} \leq 1$ and $-1 \leq \tilde{b} \leq 1$. The details of this transformation are presented in Appendix 2. Using the transformation in Equation (33), the objective function in Equation (29) can be expressed as,

$$\Phi(\mathbf{x}^c) = \sum_{i=1}^5 w_i \Upsilon_i(\mathbf{x}^c), \quad (34)$$

where $\mathbf{x}^c = (\tilde{\lambda}_1, \tilde{\lambda}_2, \tilde{a}, \tilde{b})$. To further simplify this complex nonlinear optimization, CIM proceeds sequentially. Starting with a suitably selected random solution, CIM first finds the best fit for m_1 . This is achieved by setting $w_1 = 1$ and all other weights to 0. The resulting solution is used as a starting point with $w_1 = 1, w_2 = 1 - |\text{CVC}|$ and all other weights set to 0 to fit m_1 and m_2 . The resulting solution is again used as the starting point of the next stage where m_3 is given a weight of $w_3 = 1 - |\text{CVC}|$. Similarly, the new solution is used as a starting point for the following stage where $w_4 = |\text{CVC}|$ and then again used as the starting point to the following stage where $w_5 = |\text{CVC}|$.

After the end of the sequential optimization, the termination conditions of CIM are checked. These conditions are in three folds. First, to guarantee a reasonable fit, a maximum tolerance ϵ_m is imposed on the maximum percent deviation of the first moment. Second, to improve the quality of the fit, a maximum tolerance ϵ on the value of the objective value, Φ^* , is imposed. Third, to limit the CPU time, especially in cases where a MAP(2) does not provide an accurate fit to the selected characteristics, we impose a limit, l_{\max} , on the number of iterations of the algorithm. If either one of

these three conditions are not met, the algorithm restarts with a new initial solution generated randomly. Note that the complexity of the nonlinear optimization at hand, which is inherited from the involved expressions for $m_i(\mathbf{x}), i = 1, 2, 3$, Equation (27) and $IDC(\tau; \mathbf{x})$ in Theorem 2, makes the quality of the CIM results dependent on the starting solution. The termination criteria based on ϵ_m and ϵ guarantee that a good solution is reached despite this dependency on the initial solution.

The detailed CIM algorithm is presented below. Step 0 estimates the key characteristics of the point process from raw data. Step 1 initializes the algorithm as follows. The coefficient of variation, \widetilde{scv} , of the raw data is found. If $\widetilde{scv} > 1$, the transition rates, $\widetilde{\lambda}_1$ and $\widetilde{\lambda}_2$, are initialized based on sampling from the hyper-exponential distribution. Otherwise, $\widetilde{\lambda}_1$ and $\widetilde{\lambda}_2$ are initialized based on sampling from the exponential distribution. The other MAP(2) parameters, \widetilde{a} and \widetilde{b} , are initialized based on uniform random numbers. Step 2 sets the appropriate weights and performs one step of the sequential optimization process described above. Step 3 checks whether the sequential optimization for one starting solution is completed. Finally, Step 4 checks the termination criteria in terms of meeting the tolerance level on both the first moment and the objective value. If these criteria are not met, the algorithm restarts at Step 1. Otherwise, the algorithm terminates.

4.3. CIM Algorithm

Step 0 (Estimating point process characteristics from raw data and initializing the solution set X).

- Compute $\widetilde{m}_1, \widetilde{m}_2, \widetilde{m}_3$ from the source process.
- Compute $\widetilde{IDC}(\tau_s, j)$ for $j = 1, \dots, k$ and $\widetilde{IDC}(\tau_\ell)$ from source process.
- Compute \widetilde{CVC} from source process.
- Set $l = 0$.

Step 1 (Initialization)

- Set $\widetilde{scv} = \frac{\widetilde{m}_2 - \widetilde{m}_1^2}{\widetilde{m}_1}$ (\widetilde{scv} is the squared coefficient of variation).
- If $\widetilde{scv} > 1$, then set $q = \frac{[1 + \sqrt{(\widetilde{scv}-1)/(\widetilde{scv}+1)}]}{2}$, $r_1 = \frac{2q}{\widetilde{m}_1}$, and $r_2 = \frac{2(1-q)}{\widetilde{m}_1}$.
- Else, set $q = 0.5$ and $r_1 = r_2 = \frac{1}{\widetilde{m}_1}$.
- Generate two hyper-exponential random variates, H_1 and H_2 , with parameters (q, r_1, r_2) .
- Generate one Uniform (0,1) random number U_1 , and another Uniform(-1, 1) random number U_2 .
- Set $\widetilde{\lambda}_1 = 1/\min(H_1, H_2)$, $\widetilde{\lambda}_2 = 1/\max(H_1, H_2)$, $\widetilde{a} = U_1$ and $\hat{b} = U_2$.
- Set $\mathbf{x}_0 = \{\widetilde{\lambda}_1, \widetilde{\lambda}_2, \widetilde{a}, \hat{b}\}$.

- Set $\Phi^* = M$, where M is a large number.
- Set $w_1 = w_2 = w_3 = w_4 = w_5 = 0$.
- Set $l = l + 1$.
- Set $i = 1$.

Step 2 (Set the weights and solve the corresponding sequential optimization)

- If $i = 1$, then set $w_i = 1$,
- If $i = 2, 3$, then set $w_i = 1 - |\text{CVC}|$
- If $i = 4, 5$, then set $w_i = |\text{CVC}|$
- Solve for $\mathbf{x}_1 = \arg\min_{\mathbf{x}^c} \Phi(\mathbf{x}^c)$ with \mathbf{x}_0 being the starting solution (the transformation in Equation (33) is used to calculate the characteristics).

Step 3 (Check whether the sequential optimization is done)

- If $i < 5$, then set $i = i + 1$, $\mathbf{x}_0 = \mathbf{x}_1$ and go to Step 2.

Step 4 (Save the best solution and check the termination conditions)

- If $|\frac{m_1(\mathbf{x}_1) - m_1}{m_1}| > \epsilon_m$, then go to Step 1.
- If $\Phi(\mathbf{x}_1) < \Phi^*$, then set $\mathbf{x}^* = \mathbf{x}_1$ and $\Phi^* = \Phi(\mathbf{x}_1)$.
- If $\Phi^* > \epsilon$ and $l \leq l_{\max}$, then go to Step 1,
- Else, return \mathbf{x}^* and $\Phi(\mathbf{x}^*)$.

Note that the fitting algorithm presented in this work is tailored for the MAP(2), but can be extended to the MAP(n) case by simply increasing the number of decision variables as denoted by the MAP(n) parameters. This is illustrated in Section 5.2.

5. Performance of the CIM algorithm

We compare our fitting algorithm against four existing approaches. The first approach fits a phase-type distribution to the inter-arrival time and captures the lag correlation by a MAP while maintaining the inter-arrival distribution.^[16] We refer to this algorithm as the Ph-type to MAP (PM) algorithm. The second approach fits a MAP to the inter-arrival mean and coefficient of variation as well as the correlation decay coefficient (DC).^[10] We refer to this algorithm by the DC algorithm. The third approach fits a MAP(2) to the inter-arrival moments and lag correlation.^[5] We refer to this algorithm as the Canonical or Euclidean Distance (CED) algorithm. The fourth approach utilizes the expectation maximization algorithm to fit the parameters of a MAP.^[21] We refer to the estimation approach by the EM algorithm.

To test the accuracy of our fitting algorithm, we use the resulting approximate MAP(2) from each approach as an input to a queuing system with exponential service time, one server and finite capacity, MAP(2)/M/1/ k system. We choose the MAP(2)/M/1/100 average-number-in-system as our measure of accuracy. Numerical examples are presented in the following sections, wherein Section 5.1 we fit an approximate MAP(2), via CIM, PM, DC,

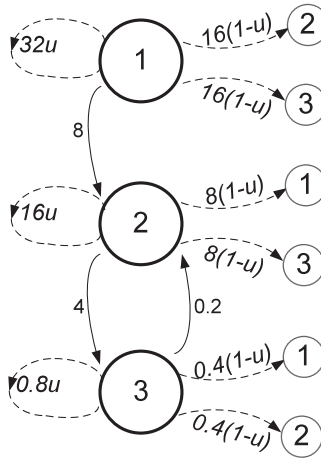


Figure 1. Numerical example – MAP(3) source process.

CED and EM, to the characteristics of higher order MAPs (MAP(3) and MAP(4)). In section 5.2, we investigate the applicability of the CIM algorithm in fitting higher order MAPs, specifically MAP(3).

5.1. Numerical examples, fitting MAP(2)s to higher order MAPs

We consider two examples where the source process in Section 5.1.1 is MAP(3) and the source process in Section 5.1.2 is MAP(4). The resulting fitted MAP(2) processes are used as the arrival process to a MAP(2)/M/1/k queuing node for $k = 100$. As a goodness of fit measure we compute the absolute percentage error between the actual average number-in-system, NS, and the approximated, \hat{NS} . The number-in-system measures, NS and \hat{NS} , are computed by solving the MAP(2)/M/1/k KFEs at steady state. We also compute the absolute percentage error between the standard deviation of the actual number-in-system, SD, and the approximated, \hat{SD} . We refer to the absolute percentage errors for the mean and standard deviations by APE_m and APE_s , respectively,

$$APE_m = \frac{|NS - \hat{NS}|}{NS} \times 100\%, \quad APE_s = \frac{|SD - \hat{SD}|}{SD} \times 100\%. \quad (35)$$

We also consider characteristics of the point processes which are not directly fitted by the optimization algorithms. We choose the fourth dimensionless standardized inter-arrival moment (see Bodrog et al.^[5]) as a goodness of fit measure, $n_k = \frac{m_k}{m_3 m_1}$. Let APE_{n_4} be the absolute percentage error for the fourth standardized inter-arrival moment.

$$APE_{n_4} = \frac{|n_4 - \hat{n}_4|}{n_4} \times 100\%. \quad (36)$$

Table 1. MAP(3) cases.

Case	u	m_1	m_2	m_3	lag-1	c_v^2	κ_1	κ_2	κ_3	IDC				CVC (%)
										$\tau_{s,1}$	$\tau_{s,2}$	$\tau_{s,3}$	τ_ℓ	
1	0.10	0.458	0.909	2.84	-0.092	3.33	0.09	0.25	0.62	1.46	1.93	2.39	2.85	-14.5
2	0.2	0.46	0.913	2.852	-0.052	3.32	0.10	0.27	0.68	1.5	2.01	2.51	3.02	-9.1
3	0.3	0.462	0.918	2.868	-0.013	3.3	0.11	0.29	0.74	1.55	2.11	2.66	3.21	-2.5
4	0.4	0.466	0.925	2.89	0.026	3.27	0.12	0.33	0.82	1.61	2.22	2.84	3.45	5.3
5	0.5	0.47	0.935	2.921	0.064	3.23	0.13	0.36	0.91	1.68	2.37	3.05	3.73	13.6
6	0.6	0.477	0.95	2.968	0.101	3.17	0.15	0.41	1.03	1.77	2.54	3.31	4.08	22.3
7	0.7	0.489	0.974	3.043	0.136	3.08	0.17	0.47	1.17	1.87	2.74	3.62	4.49	31.5
8	0.8	0.509	1.016	3.177	0.167	2.92	0.2	0.53	1.33	1.99	2.97	3.95	4.94	40.8
9	0.9	0.55	1.103	3.448	0.188	2.65	0.22	0.59	1.47	2.06	3.12	4.18	5.25	49.4

We also consider the average absolute percentage error for the joint moments, $AAPE_{jm}$,

$$AAPE_{jm} = \frac{1}{h} \sum_{i=1}^h \left(\frac{|E[X_0 X_i] - E[\hat{X}_0 X_i]|}{E[X_0 X_i]} \times 100\% \right). \tag{37}$$

In the numerical examples sections we calculate the $AAPE_{jm}$ over the first 10 joint moments, $h = 10$. The equations to calculate the count and inter-arrival moments for a MAP(n) are presented in Sections 2.2 and 2.4. The inter-arrival moments are calculated by solving Equations (19) and (20) for $k = 1, 2, 3, 4$. The count moments are calculated using Equations (7), (8) and (10).

5.1.1. Numerical examples with MAP(3) source process

We consider MAP(3) cases with a fixed structure (see Figure (1)), and parameters stated below according to the following matrix representation,

$$D_0 = \begin{pmatrix} -40 & 8 & 0 \\ 0 & -20 & 4 \\ 0 & 0.2 & -1 \end{pmatrix} \text{ and } D_1 = \begin{pmatrix} 32u & 16(1-u) & 16(1-u) \\ 8(1-u) & 16u & 8(1-u) \\ 0.4(1-u) & 0.4(1-u) & 0.8u \end{pmatrix}.$$

The parameter u is varied according to Table 1 where the resulting characteristics are reported. Notice that increasing the value of the parameter u (as shown in Figure 1) does not change the departure rate from a state but impacts the one step probabilities. Specifically, increasing the parameter u increases the one step transition probability of returning to the departing state, $P_{i,i}$ for $i = 1, 2$ and 3 , which increases the inter-arrival correlation. Consequently, as the parameter u increases, the CVC increases.

The APE_m is calculated in Tables 11 and 12 of Appendix 5, for the MAP(3) cases using the CIM, PM, DC and CED algorithms, where the traffic intensities (ρ) are 0.6 and 0.9. Tables 2 and 3 are a summary of the results where the average absolute percentage error, Avg. APE_m , of the CIM over the MAP(3) cases for $\rho = 0.9$ is 1.36% compared to 2.72% for

Table 2. Summary of results for mean number-in-system – MAP(3).

	APE _m (ρ=.6)					APE _m (ρ=.9)				
	CIM (%)	PM (%)	DC (%)	CED (%)	EM (%)	CIM (%)	PM (%)	DC (%)	CED (%)	EM (%)
AVG	1.70	2.98	23.96	0.31	3.76	1.36	2.72	22.18	0.15	5.94
MIN	0.11	0.33	0.07	0.00	0.42	0.09	0.31	0.08	0.00	0.39
MAX	4.38	6.83	92.26	1.50	8.19	3.79	7.44	87.66	0.74	22.16

Table 3. Summary of results for St. deviation of number-in-system - MAP(3).

	APE _s (ρ=.6)					APE _s (ρ=.9)				
	CIM (%)	PM (%)	DC (%)	CED (%)	EM (%)	CIM (%)	PM (%)	DC (%)	CED (%)	EM (%)
AVG	2.15	2.92	26.21	0.45	4.37	1.16	1.87	17.16	0.14	4.68
MIN	0.12	0.33	0.08	0.00	0.38	0.08	0.22	0.06	0.00	0.63
MAX	5.26	6.84	100.8	2.20	10.57	3.27	5.15	61.87	0.66	19.69

Table 4. Summary of results for distribution characteristics - MAP(3).

	APE _{n_a}					AAPE _{j_m}				
	CIM (%)	PM (%)	DC (%)	CED (%)	EM (%)	CIM (%)	PM (%)	DC (%)	CED (%)	EM (%)
AVG	0.19	0.95	82.96	0.02	10.35	0.70	0.52	1.77	0.07	1.76
MIN	0.03	0.03	0.00	0.01	0.07	0.03	0.03	0.02	0.00	0.46
MAX	0.38	2.14	498.59	0.02	65.4	2.40	1.21	7.19	0.33	4.20

PM, 22.18% for DC, 0.15% for CED and 5.94% for EM. Also, for ρ = 0.9, the average absolute error for the standard deviation, Avg. APE_s, for the CIM is 1.16% compared to 1.87, 17.16, 0.14 and 4.68% for the PM, DC, CED and EM algorithms, respectively.

The nonlinear optimization algorithm of Step 5 is implemented using a solver in MATLAB for the numerical examples presented in this article. The solver is based on a line search *via* a Quasi-Newton approach. The average convergence time of the optimization algorithm is 5.92 s over the 9 MAP(3) cases. This convergence is based on error bounds on the mean and objective value of ε_m = 0.001 and ε = 0.0001, respectively, and a maximum number of allowable iterations l_{max} = 100. We point that the maximum number of iterations l_{max} was not reached for the 9 MAP(3) cases. Next we consider an example where the underlying distribution is a MAP(4).

5.1.2. Numerical examples with MAP(4) source process

Similarly, the MAP(4) cases considered have a fixed structure (see Figure 2), with the following parameters.

$$D_0 = \begin{pmatrix} -30 & 30 & 0 & 0 \\ 0 & -30 & 30 & 0 \\ 0 & 0 & -30 & 0 \\ 0 & 0 & 0 & -4 \end{pmatrix} \text{ and } D_1 = \begin{pmatrix} 0 & 0 & 0 & 0 \\ 0 & 0 & 0 & 0 \\ 30u & 0 & 0 & 30(1-u) \\ 4(1-u) & 0 & 0 & 4u \end{pmatrix}.$$

Increasing the parameter *u* increases the inter-arrival correlation and consequently increases the CVC.

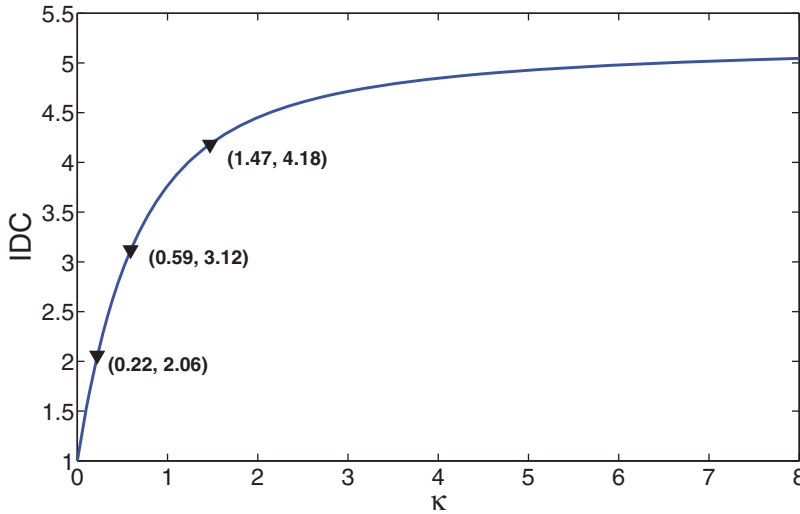


Figure 2. Numerical example – MAP(4) source process.

The parameter u is varied according to Table 5 where the resulting characteristics are reported. The values for the resulting inter-arrival moments of the cases in Table 5 are $m_1 = 0.175$, $m_2 = 0.069$ and $m_3 = 0.048$ with squared coefficient of variation $c_v^2 = 1.259$.

Tables 13 and 14 of Appendix 5 present the APE_m for the considered MAP(4) cases using the CIM, PM, DC, CED and EM algorithms. Tables 6 and 7 are a summary of the results. The average absolute percentage error of the CIM over the MAP(4) cases for $\rho = 0.9$ is 3.92% compared to 17.43% for PM, 4.56% for DC, 31.83% for CED and 25.58% for EM. Also, the absolute percentage error, APE_s , for the CIM is 4.15% which is lower than the APE_s for PM, DC, CED and EM (14.79, 4.80, 18.10 and 25.99%, respectively). For the MAP(4) cases, the CIM algorithm converged to the target limits of the error bounds, of $\epsilon_m = 0.001$ and $\epsilon = 0.0001$, in four cases, with an average CPU time of around one minute. In the other cases, the algorithm terminated after reaching the maximum number of iterations $l_{\max} = 100$, with an average CPU time of around 2 m.

5.1.3 MAP(3) and MAP(4) cases - Performance Summary

As reported in Tables 2–4, the most accurate fits are produced via the CED algorithm, although the three algorithms CIM, PM and CED perform well for the MAP(3) cases where the highest average APE_m out of the three is 2.98% and the highest average APE_s is 2.92%. The three algorithms also perform well when fitting the distribution characteristics, n_4 , and the joint moments as can be seen in Table 4. Although the EM did not provide accurate results when utilizing the queuing node number in system as the performance measure (Tables 6 and 7), it provided a better match than the

Table 5. MAP(4) cases.

Case	u	lag-1	κ_1	κ_2	κ_3	IDC				CVC (%)
						$\tau_{s,1}$	$\tau_{s,2}$	$\tau_{s,3}$	τ_t	
1	0.1	-0.117	0.91	1.44	2.89	0.92	0.98	1.04	1.10	-13.0
2	0.2	-0.088	0.12	1.55	3.13	0.93	0.99	1.06	1.12	-10.9
3	0.3	-0.058	1.01	1.68	3.43	0.94	1.01	1.08	1.15	-8.3
4	0.4	-0.029	1.09	1.86	3.84	0.95	1.03	1.11	1.20	-4.9
5	0.5	0.000	1.19	2.09	4.39	0.96	1.06	1.16	1.26	0.0
6	0.6	0.029	1.33	2.44	5.21	0.99	1.11	1.23	1.35	6.8
7	0.7	0.058	1.56	3.01	6.57	1.02	1.18	1.34	1.50	16.3
8	0.8	0.088	2.01	4.13	9.26	1.10	1.34	1.57	1.81	30.5
9	0.9	0.117	3.29	7.41	17.29	1.33	1.80	2.26	2.73	53.9

Table 6. Summary of results for mean number-in-system - MAP(4).

	APE _m ($\rho=.6$)					APE _m ($\rho=.9$)				
	CIM (%)	PM (%)	DC (%)	CED (%)	EM (%)	CIM (%)	PM (%)	DC (%)	CED (%)	EM (%)
AVG	3.02	4.14	4.99	4.82	13.27	3.92	17.43	4.56	31.83	28.58
MIN	0.13	0.54	0.11	0.59	2.42	0.20	0.05	0.96	0.06	2.24
MAX	5.21	7.76	11.44	9.84	41.15	6.94	108.3	10.93	249.0	76.1

Table 7. Summary of results for St. deviation of number-in-system - MAP(4).

	APE _s ($\rho=.6$)					APE _s ($\rho=.9$)				
	CIM (%)	PM (%)	DC (%)	CED (%)	EM (%)	CIM (%)	PM (%)	DC (%)	CED (%)	EM (%)
AVG	3.95	4.69	6.46	5.72	15.5	4.15	14.79	4.80	18.10	25.99
MIN	0.76	0.31	0.61	0.36	3.03	0.21	0.03	0.91	0.04	2.65
MAX	7.44	8.57	16.81	11.04	45.18	7.15	85.15	11.61	125.1	68.68

CIM algorithm for the fourth standardized inter-arrival moment characteristic APE_{n_4} as shown in Table 8. We also point out that while running the EM algorithm, the convergence is very slow and highly dependent on the starting solution. These observations are also stated in Kriege and Buchholz,^[23] Horvath and Okamura,^[17] and Buchholz and Panchenko.^[8] In the MAP(4) set of examples, the CIM significantly outperforms the CED and PM for high traffic intensities, see Tables 6 and 7. The four algorithms perform well when fitting the joint moments as can be seen in Table 8. The performance of the PM, DC and CED algorithms is similar for the standardized characteristic n_4 but the APE_{n_4} is higher for the CIM algorithm, 18%, as can be seen in Table 8.

To summarize the queuing performance of both sets of MAP(3) and MAP(4) numerical examples, the CIM algorithm performed relatively well with a maximum APE_m of 7.44% overall cases. The DC algorithm performed well in general except for a few MAP(3) cases (cases 1, 2 and 3). The CED and PM algorithms performed well for all cases except for the high traffic set of MAP(4) examples where the average APE_m for the algorithms is 18.10 and 14.79%, respectively.

Table 8. Summary of results for distribution characteristics - MAP(4).

	APE _{n_a}					AAPE _{j_m}				
	CIM (%)	PM (%)	DC (%)	CED (%)	EM (%)	CIM (%)	PM (%)	DC (%)	CED (%)	EM (%)
AVG	18.01	6.12	8.04	7.54	11.73	1.67	1.79	0.89	3.52	12.11
MIN	1.40	1.14	3.42	2.15	0.37	0.01	0.00	0.04	0.00	2.40
MAX	31.52	9.72	10.43	9.68	30.94	6.72	6.32	4.74	11.33	76.09

Table 9. Summary of results for mean and St. deviation of number-in-system.

	$\rho=.6$				$\rho=.9$			
	APE _m		APE _s		APE _m		APE _s	
	MAP(2) (%)	MAP(3) (%)	MAP(2) (%)	MAP(3) (%)	MAP(2) (%)	MAP(3) (%)	MAP(2) (%)	MAP(3) (%)
AVG	3.02	1.99	3.95	2.68	3.92	1.36	4.15	1.50
MIN	0.13	0.26	0.76	0.57	0.20	0.37	0.21	0.55
MAX	5.21	3.66	7.44	4.89	6.94	3.45	7.15	3.98

Table 10. Summary of results for distribution characteristics.

	APE _{n_a}		AAPE _{j_m}	
	MAP(2) (%)	MAP(3) (%)	MAP(2) (%)	MAP(3) (%)
AVG	18.01	3.29	1.67	0.80
MIN	1.40	0.48	0.01	0.00
MAX	31.52	23.03	6.72	6.77

5.2. Applications of the CIM on the higher order MAP(3)

The CIM approach can be extended to fit higher-order MAPs by providing efficient approaches to calculate the inter-arrival moments as well as the moments of the counting process over any time interval of duration t . The calculation of inter-arrival moments and the moments of the counting process is done as discussed in Sections 2.4 and 2.2, respectively. In this work we also present, in Section, a computationally efficient approach to calculate Accordingly, the CIM approach can be efficiently extended to fit higher-order MAPs. We reconsider the MAP(4) cases as presented in Table 5 and we fit the MAP(4) key characteristics to a MAP(3) by applying the CIM approach. Tables 9 and 10 below summarize the performance of the CIM algorithm where the approximating process is a MAP(3), CIM-MAP(3), and the approximating process is a MAP(2), CIM-MAP(2) (Table 15 in Appendix 5 presents the detailed results).

As expected, the numerical examples illustrate that the CIM-MAP(3) algorithm provides a superior fit over the CIM-MAP(2) approach. Furthermore, the fitted MAP(3) provides the smallest approximation error for all the performance measure criteria (APE_m , APE_s , APE_m , APE_{n_a} and $AAPE_{j_m}$) and overall the MAP(3) fitting and estimation approaches considered in Tables 6 and 8 of this work.

6. Conclusion

This article develops and tests an algorithm that fits two phase MAP(2), to correlated point processes by fitting moments of inter-arrivals and counts. The fitted point processes are generated using the more general MAP(3) and (4) distributions. The CIM algorithm yields superior fits when compared to other algorithms in the literature that fit inter-arrival moments and lag correlations. This illustrates that matching count characteristics provides a good fit to a correlated point process.

This article serves as a starting point to efficiently fit higher-order MAPs to point processes using count and inter-arrival moments, especially that this paper presents an effective computational framework for evaluating the moments of counts and inter-arrival times of the general MAP(n). We illustrate that the approach presented in this article can be easily tailored to higher order MAPs by fitting a MAP(3) in a set of numerical examples. Our numerical examples focus on investigating and benchmarking the goodness of fit of the CIM algorithm at different process correlation levels as measured by the CVC.

We also note that the algorithm presented in this work allows for fitting a weighted combination of the key characteristics which can be adjusted to include third order or higher descriptors. For example, the approach implemented in this article is not limited to a weighted combination of the first two orders but includes the third inter-arrival moment. Future work can include investigating the effectiveness of using a weighted combination of higher order moments to fit MAP(n) for $n > 2$. Such higher order moments can include cross moment based on intervals/counts as defined in Andersen et al.^[2] Finally, we observe numerically that our moment matching algorithm performs generally better than the EM method^[21] especially in terms of accurate estimation of performance measures for a queuing system. This is contrast to the common belief that EM approaches provide better fits. In future research, it will be interesting to investigate this observation further. In particular, it is important to verify whether the unexpected EM performance is due to the computational difficulty of finding the maximum of the complex likelihood function, or to a more fundamental cause.¹

Disclosure statement

No potential conflict of interest was reported by the authors.

¹We thank an anonymous reviewer for suggesting this future research direction.

References

- [1] Albin, S.L. Approximating a point process by a renewal process II: superposition arrival processes to queues. *Oper. Res.* **1984**, *32*, 1133–1162.
- [2] Andersen, A.T.; Neuts, M.F.; Friis Nielsen, B. On the time reversal of Markovian arrival processes. *Stoch. Models* **2004**, *20*, 237–260.
- [3] Andersen, A.T.; Nielsen, B.F. On the use of second-order descriptors to predict queueing behavior of MAPs. *Nav. Res. Logist.* **2002**, *49*, 391–409.
- [4] Begin, T.; Brandwajn, A. *A Note on the Accuracy of Several Existing Approximations for M/Ph/m Queues*, Computer Software and Applications Conference Workshops (COMPSACW), 2013 IEEE 37th Annual, IEEE: Torino, Italy, **2013**; 730–735.
- [5] Bodrog, L.; Buchholz, P.; Krieger, J.; Telek, M. *Canonical form Based MAP(2) Fitting*, Proceedings of the 7th International Conference on the Quantitative Evaluation of Systems, QEST: Williamsburg, Virginia, **2010**; 107–116.
- [6] Bodrog, L.; Heindl, A.; Horvath, G.; Telek, M. A markovian canonical form of second-order matrix-exponential processes. *Eur. J. Oper. Res.* **2008**, *190*, 459–477.
- [7] Buchholz, P.; Krieger, J.; Felko, I. *Input Modeling with Phase-Type Distributions and Markov Models Theory and Applications*; Berlin, Germany: Springer, **2014**.
- [8] Buchholz, P.; Panchenko, A. A two-step EM algorithm for MAP fitting. In *International Symposium on Computer and Information Sciences*; Heidelberg, Germany: Springer Berlin Heidelberg, **2004**; 217–227.
- [9] Cox, D.R.; P. A. W. Lewis. *The Statistical Analysis of Series of Events*; London: Chapman and Hall, **1966**.
- [10] Diamond, J.; Alfa, A. On approximating higher order MAPs with MAPs of order two. *Queueing Syst.* **2000**, *34*, 269–288.
- [11] Fischer, F.; Meier-Hellstern, K. The Markov-modulated poisson process (MMPP) cook-book. *Perform. Eval.* **1992**, *18*, 149–171.
- [12] Gusella, R. Characterizing the variability of arrival processes with indexes of dispersion. *IEEE J. Select. Areas Commun.* **1991**, *9*, 203–211.
- [13] Feldmann, A.; Whitt, W. Fitting mixtures of exponentials to long-tail distributions to analyze network performance models. *Perform. Eval.* **1998**, *31*, 245–279.
- [14] Gast, N.; Van Houdt, B. TTL Approximations of the cache replacement algorithms LRU (m) and h-LRU. *Perform. Eval.* **2017**, *117*, 33–57.
- [15] Heffes, H.; Lucantoni, D.M. A Markov modulated characterization of packetized voice and data traffic and related statistical multiplexer performance. *IEEE J. Select. Areas Commun.* **1986**, *4*, 856–868.
- [16] Horvath, G.; Buchholz, P.; Telek, M. *A MAP fitting approach with independent approximation of the inter-arrival time distribution and the lag correlation*, Second International Conference on the Quantitative Evaluation of Systems, IEEE: Torino, Italy, **2005**; 124–133.
- [17] Horvath, G.; Okamura, H. A fast EM algorithm for fitting marked Markovian arrival processes with a new special structure. In *European Workshop on Performance Engineering*; Heidelberg, Germany: Springer Berlin Heidelberg, **2013**; 119–133.
- [18] Heindl, A.; Mitchell, K.; van de Liefvoort, A. Correlation bounds for second-order MAPs with application to queueing network decomposition. *Perform. Eval.* **2006**, *63*, 553–577.
- [19] Johnson, M.A.; Luhman, J. A. Behaviour of queueing approximations based on sample moments. *Appl. Stochastic Models Data Anal.* **1994**, *10*, 233–246.

- [20] Kim, S. The characteristic polynomial and the Laplace representations of MAP(2)s. *Stoch. Models* **2016**, *1*, 18.
- [21] Klemm, A.; Lindemann, C.; Lohmann, M. Modeling IP traffic using the batch Markovian arrival process. *Perform. Eval.* **2003**, *54*, 149–173.
- [22] Kriege, J.; Buchholz, P. An empirical comparison of MAP fitting algorithms. *Lecture Notes in Computer Science*; Switzerland: Springer, **2010**; 259–273.
- [23] Kriege, J.; Buchholz, P. PH and MAP fitting with aggregated traffic traces. In *Measurement, Modelling, and Evaluation of Computing Systems and Dependability and Fault Tolerance*; Switzerland: Springer International Publishing, **2014**; 1–15.
- [24] Lucantoni, D.M.; Meier-Hellstern, K.S.; Neuts, M. A single-server queue with server vacations and a class of non-renewal arrival processes. *Adv. Appl. Probab.* **1990**, *22*, 676–705.
- [25] Narayana, S.; Neuts, M. The first two moment matrices of the counts for the Markovian arrival process. *Stoch. Models* **1992**, *8*, 459–477.
- [26] Nasr, W.W.; Elshar, I.J. Continuous inventory control with stochastic and non-stationary markovian demand. *Eur. J. Oper. Res.* **2018**, *270*, 198–217. <https://doi.org/10.1016/j.ejor.2018.03.023>.
- [27] Nasr, W.W.; Maddah, B. Continuous (s, S) policy with MMPP correlated demand. *Eur. J. Oper. Res.* **2015**, *246*, 874–885.
- [28] Nasr, W.; Taaffe, M. Fitting the $Ph_t/M_t/s/c$ time-dependent departure process for use in tandem queueing networks. *INFORMS J. Comput.* **2013**, *25*, 758–773.
- [29] Nelson, B.; Gerhardt, I. *On Capturing Dependence in Point Processes: Matching Moments and Other Techniques*. Technical Report; Evanston, IL: Northwestern University, **2010**.
- [30] Nielsen, B.F.; Nilsson, L.F.; Thygesen, U.H.G.; Beyer, J. E. Higher order moments and conditional asymptotics of the batch Markovian arrival process. *Stoch. Models* **2007**, *23*, 1–26.
- [31] Neuts, M. A versatile Markovian point process. *J. Appl. Probab.* **1979**, *16*, 764–779.
- [32] Neuts, M.F.; Li, J.M. *An algorithm for the $P(n,t)$ matrices of a continuous BMAP*; Abingdon: Taylor and Francis Group, **1996**.
- [33] Okamura, H.; Dohi, T.; Trivedi, K. Markovian arrival process parameter estimation with group data. *IEEE/ACM Trans. Network.* **2009**, *17*, 1326–1339.
- [34] Ramirez-Cobo, P.; Carrizosa, E. A note on the dependence structure of the two-state Markovian arrival process. *J. Appl. Probab.* **2012**, *49*, 295–302.
- [35] Rodriguez, J.; Lillo, R.E.; Ramirez-Cobo, P. Dependence patterns for modeling simultaneous events. *Reliabil. Eng. Syst. Safe.* **2016**, *154*, 19–30.
- [36] Sahin, I.; Perrakis, S. Moment inequalities for a class of single server queues. *INFOR: Inform. Syst. Oper. Res.* **1976**, *14*, 144–152.
- [37] Sivakumar, B.; Arivarignan, G. A stochastic inventory system with postponed demands. *Perform. Eval.* **2009**, *66*, 47–58.
- [38] Smith, W. On the cumulants of renewal processes. *Biometrika* **1959**, *46*, 502–529.
- [39] Sriram, K.; Whitt, W. Characterizing superposition arrival processes in packet multiplexers for voice and data. *IEEE J. Select. Areas Commun.* **1986**, *4*, 833–846.
- [40] Telek, M.; Horvath, G. A minimal representation of Markov arrival processes and a moments matching method. *Perform. Eval.* **2007**, *64*, 1153–1168.
- [41] Whitt, W. Approximating a point process by a renewal process, I: two basic methods. *Oper. Res.* **1982**, *30*, 125–147.
- [42] Whitt, W. The queueing network analyzer. *Bell Syst. Tech. J.* **1983**, *62*, 2779–2815.

- [43] Whitt, W. On approximations for queues, III: mixtures of exponential distributions. *Bell Lab. Tech. J.* **1984**, *63*, 163–175.
- [44] Van Loan, C. Computing integrals involving the matrix exponential. *IEEE Trans. Automat. Contr.* **1978**, *23*, 395–404.
- [45] Zheng, J.; Okamura, H.; Li, L.; Dohi, T.A. Comprehensive evaluation of software rejuvenation policies for transaction systems with Markovian arrivals. *IEEE Trans. Rel.* **2017**, *66*, 1157–1177.

Appendix 1: Derivation of MAP(n) count PMDEs

Substituting the KFEs of Equation 1 in Equation 3,

$$\begin{aligned}
 E' \left[C_t^k(\tau), A(t+\tau) = \ell \right] &= \sum_{c=1}^{\infty} c^k P'_{\ell,c} \\
 &= - \sum_{c=1}^{\infty} c^k \sigma_{\ell} P_{\ell,c} + \sum_{c=1}^{\infty} c^k \sum_{i=1, i \neq \ell}^n \alpha_{i,\ell} P_{i,c} + \sum_{c=1}^{\infty} c^k \sum_{i=1}^n \lambda_{i,\ell} P_{i,c-1} \\
 &= -\sigma_{\ell} E \left[C_t^k(\tau), A(t+\tau) = \ell \right] + \sum_{i=1, i \neq \ell}^n \alpha_{i,\ell} E \left[C_t^k(\tau), A(t+\tau) = i \right] \\
 &\quad + \sum_{i=1}^n \lambda_{i,\ell} \left(\sum_{c=1}^{\infty} c^k P_{i,c-1} \right).
 \end{aligned} \tag{38}$$

The following term appearing on the right hand side of Equation (38) is expanded,

$$\begin{aligned}
 \sum_{i=1}^n \lambda_{i,\ell} \left(\sum_{c=1}^{\infty} c^k P_{i,c-1} \right) &= \sum_{i=1}^n \lambda_{i,\ell} \left(\sum_{c=0}^{\infty} (c+1)^k P_{i,c} \right) = \sum_{i=1}^n \lambda_{i,\ell} \left(\sum_{c=0}^{\infty} \sum_{j=0}^k \binom{k}{j} c^j P_{i,c} \right) \\
 &= \sum_{i=1}^n \lambda_{i,\ell} \left(\sum_{j=0}^k \binom{k}{j} E \left[C_t^j(\tau), A(t+\tau) = i \right] \right) \\
 &= \sum_{i=1}^n \lambda_{i,\ell} \left(\sum_{j=1}^k \binom{k}{j} E \left[C_t^j(\tau), A(t+\tau) = i \right] + P(A(t+\tau) = i) \right).
 \end{aligned} \tag{39}$$

Combining Equation (38) with Equation (39) results in Equation (4).

Appendix 2: MAP(2) transformation

We refer to Bodrog et al.^[6] for details on the definition of the general canonical form. Two representations of the canonical form are presented in Bodrog et al.^[6] The first canonical MAP(2) representation when $\tilde{\gamma} > 0$,

$$\mathbf{D}_0 = \begin{pmatrix} -\tilde{\lambda}_1 & (1-\tilde{a})\tilde{\lambda}_1 \\ 0 & -\tilde{\lambda}_2 \end{pmatrix}, \text{ and } \mathbf{D}_1 = \begin{pmatrix} \tilde{a} \tilde{\lambda}_1 & 0 \\ (1-\tilde{b})\tilde{\lambda}_2 & \tilde{b} \tilde{\lambda}_2 \end{pmatrix},$$

The second canonical MAP(2) representation when $\tilde{\gamma} < 0$,

$$\mathbf{D}_0 = \begin{pmatrix} -\tilde{\lambda}_1 & (1-\tilde{a})\tilde{\lambda}_1 \\ 0 & -\tilde{\lambda}_2 \end{pmatrix}, \text{ and } \mathbf{D}_1 = \begin{pmatrix} 0 & -\tilde{a} \tilde{\lambda}_1 \\ \tilde{b} \tilde{\lambda}_2 & (1-\tilde{b}) \tilde{\lambda}_2 \end{pmatrix}.$$

Also, $0 < \tilde{\lambda}_1 \leq \tilde{\lambda}_2, 0 \leq \tilde{a} \leq 1$ and $0 \leq \tilde{b} \leq 1$. We refer the reader to Bodrog et al.^[6] for further information on the representation and the additional information on the boundaries of the parameters. To further simplify the transformation we define the indicator function $I_{\tilde{\gamma}} = 1$ if $\tilde{\gamma} \geq 0$ and $I_{\tilde{\gamma}} = -1$ otherwise. Let $\hat{b} = \tilde{b} I_{\tilde{\gamma}}$. Since, $\tilde{\gamma} = \tilde{a} \tilde{b}$ if $\tilde{\gamma} \geq 0$, and $\tilde{\gamma} = -\tilde{a} \tilde{b}$ if $\tilde{\gamma} < 0$, this results in $\tilde{\gamma} = \tilde{a} \hat{b}$ and $-1 \leq \hat{b} \leq 1$. The resulting transformation can be expressed in terms of $\tilde{\lambda}_1, \tilde{\lambda}_2, \tilde{a}$ and \hat{b} as,

$$\alpha_{12} = \tilde{\lambda}_1(1-\tilde{a}), \alpha_{21} = 0, \lambda_{11} = I_{\hat{b}} \tilde{\lambda}_1 \tilde{a}, \lambda_{22} = (1-I_{\hat{b}} + \hat{b}) \tilde{\lambda}_2, \lambda_{12} = \tilde{\lambda}_1 - \lambda_{11} - \alpha_{12},$$

$$\lambda_{21} = \tilde{\lambda}_2 - \lambda_{22}$$

where the indicator function $I_{\hat{b}} = 1$ if $\hat{b} \geq 0$, and $I_{\hat{b}} = 0$ otherwise.

Appendix 3: MAP(2) count characteristics

Proof of Theorem 1. The special case where $n = 2$ for Equations (5) and (4) (for $k = 1, 2$) results with the following PMDEs for the MAP(2) case,

$$\begin{aligned} P'(A(t + \tau) = 1) &= -c_1 P(A(t + \tau) = 1) + c_2 P(A(t + \tau) = 2), \\ P'(A(t + \tau) = 2) &= -c_2 P(A(t + \tau) = 2) + c_1 P(A(t + \tau) = 1), \end{aligned} \tag{40}$$

$$\begin{aligned} E'[C_t(\tau), 1] &= -c_1 E[C_t(\tau), 1] + c_2 E[C_t(\tau), 2] \\ &\quad + \lambda_{11} P(A(t + \tau) = 1) + \lambda_{21} P(A(t + \tau) = 2), \\ E'[C_t(\tau), 2] &= -c_2 E[C_t(\tau), 2] + c_1 E[C_t(\tau), 1] \\ &\quad + \lambda_{22} P(A(t + \tau) = 2) + \lambda_{12} P(A(t + \tau) = 1), \end{aligned} \tag{41}$$

$$\begin{aligned} E'[C_t^2(\tau)] &= 2 c_3 E[C_t(\tau), 1] + 2 c_4 E[C_t(\tau), 2] \\ &\quad + c_3 P(A(t + \tau) = 1) + c_4 P(A(t + \tau) = 2), \end{aligned} \tag{42}$$

where c_1, c_2, c_3 and c_4 are as given in Theorem 1. The PMDEs presented in Equations 40–42 result in a set of closed-form expressions of the first two moments of $C(\tau)$, which are given in Theorem 1. Let P_1 and P_2 be the stationary probability of being in Phases 1 and 2 respectively. From Equation 40 we have

$$-c_1 P_1 + c_2 P_2 = 0.$$

Since $P_1 + P_2 = 1$, this results in

$$P_1 = \frac{c_2}{c_1 + c_2} = \frac{c_2}{\beta}, P_2 = \frac{c_1}{c_1 + c_2} = \frac{c_1}{\beta}. \tag{43}$$

Let $y_1(\tau) = E[C(\tau), 1], y_2(\tau) = E[C(\tau), 2]$ and $z(\tau) = E[C(\tau)^2]$ and let $Y_1(s), Y_2(s)$ and $Z(s)$ be the Laplace transforms of $y_1(\tau), y_2(\tau)$ and $z(\tau)$, respectively. The Laplace transformations of the equations in Equations (41) and (42),

$$sY_1(s) - y_1(0) = -c_1 Y_1(s) + c_2 Y_2(s) + w_1 s^{-1} \tag{44}$$

$$sY_2(s) - y_2(0) = -c_2 Y_2(s) + c_1 Y_1(s) + w_2 s^{-1} \tag{45}$$

$$sZ(s) - z(0) = 2c_3 Y_1(s) + 2c_4 Y_2(s) + (c_3 P_1 + c_4 P_2) s^{-1} \tag{46}$$

where $w_1 = \lambda_{11} P_1 + \lambda_{21} P_2$ and $w_2 = \lambda_{22} P_2 + \lambda_{12} P_1$. It can be shown that $w_1 + w_2 = c_5 + c_6 = \theta_2/\beta$. Solving Equations (44–46) with $y_1(0) = y_2(0) = z(0) = 0$,

$$Y_1(s) = \frac{\theta_2 P_1 + s w_1}{s^2(s + \beta)}, Y_2(s) = \frac{\theta_2 P_2 + s w_2}{s^2(s + \beta)}, Z(s) = 2 \left(\frac{\theta_2^2/\beta + s w}{s^3(s + \beta)} \right) + \frac{\theta_2}{s^2 \beta}, \tag{47}$$

where w is given by,

$$w = c_3 w_1 + c_4 w_2. \tag{48}$$

We invert the Laplace Transformations to get,

$$E[C(\tau), 1] = \left(\frac{-w_1}{\beta} + \frac{P_1 \theta_2}{\beta^2} \right) e^{-\beta\tau} + \frac{w_1}{\beta} + \frac{P_1 \theta_2 (\beta \tau - 1)}{\beta^2}, \tag{49}$$

$$E[C(\tau), 2] = \left(\frac{-w_2}{\beta} + \frac{P_2 \theta_2}{\beta^2} \right) e^{-\beta\tau} + \frac{w_2}{\beta} + \frac{P_2 \theta_2 (\beta \tau - 1)}{\beta^2}, \tag{50}$$

Adding Equations (49) and (50) and utilizing $w_1 + w_2 = \theta_2/\beta$ results in Equation 21. It can be shown that $w = \frac{\theta_2^2}{\beta^2} - \frac{\theta_3}{2\beta}$, and after inverting the Laplace Transformation $Z(s)$,

$$E[C^2(\tau)] = \frac{\theta_1}{\beta^2} \tau + \frac{\theta_2^2}{\beta^2} \tau^2 + \frac{\theta_3}{\beta^3} (1 - e^{-\beta\tau}). \tag{51}$$

This completes the proof of Theorem 1. □

Proof of Theorem 2. The first moment and second moments of the $C(\tau)$ are presented in Theorem 1. The variance of $C(\tau)$ becomes,

Applying Equation (14), we

$$\text{Var}[C(\tau)] = E[C^2(\tau)] - E^2[C(\tau)] = \frac{\theta_1}{\beta^2} \tau + \frac{\theta_3}{\beta^3} (1 - e^{-\beta\tau}). \tag{52}$$

get Equation (24). Now, taking the limit as τ tends to ∞ , we get Equation (25). □

Appendix 4: Examples on computing the count characteristics

Example 1. MAP Parameters

$$D_0 = \begin{pmatrix} -40 & 8 & 0 \\ 0 & -20 & 4 \\ 0 & 0.2 & -1 \end{pmatrix}, \text{ and } D_1 = \begin{pmatrix} 28.8 & 1.6 & 1.6 \\ 0.8 & 14.4 & 0.8 \\ 0.04 & 0.04 & 0.72 \end{pmatrix}.$$

A plot of the IDC vs $\kappa = t/m_1$ is presented in Figure 3 for the MAP parameters of Example 1. The IDC converges to a value of $IDC(\tau_\ell) = 5.25$. Using Equation 28 for $k=3$, the corresponding points are represented by $\kappa_1 = 0.22, \kappa_2 = 0.59$ and $\kappa_3 = 1.47$ which results in $IDC(\kappa_1 m_1) = 2.06, IDC(\kappa_2 m_1) = 3.12$ and $IDC(\kappa_3 m_1) = 4.18$.

Example 2. MAP Parameters

$$D_0 = \begin{pmatrix} -30 & 30 & 0 & 0 \\ 0 & -30 & 30 & 0 \\ 0 & 0 & -30 & 0 \\ 0 & 0 & 0 & -4 \end{pmatrix} \text{ and } D_1 = \begin{pmatrix} 0 & 0 & 0 & 0 \\ 0 & 0 & 0 & 0 \\ 27 & 0 & 0 & 3 \\ 0.4 & 0 & 0 & 3.6 \end{pmatrix}.$$

A plot of the IDC vs κ is presented in Figure 4 for the MAP parameters of Example 2. The IDC converges to a value of $IDC(\tau_\ell) = 2.73$. Using Equation 28 for $k=3$, the corresponding points are represented by $\kappa_1 = 3.29, \kappa_2 = 7.41$ and $\kappa_3 = 17.29$ which results in $IDC(\kappa_1 m_1) = 1.33, IDC(\kappa_2 m_1) = 1.80$ and $IDC(\kappa_3 m_1) = 2.26$.

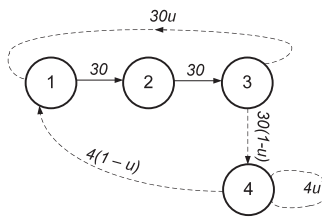


Figure 3. Example 1: IDC vs. κ .

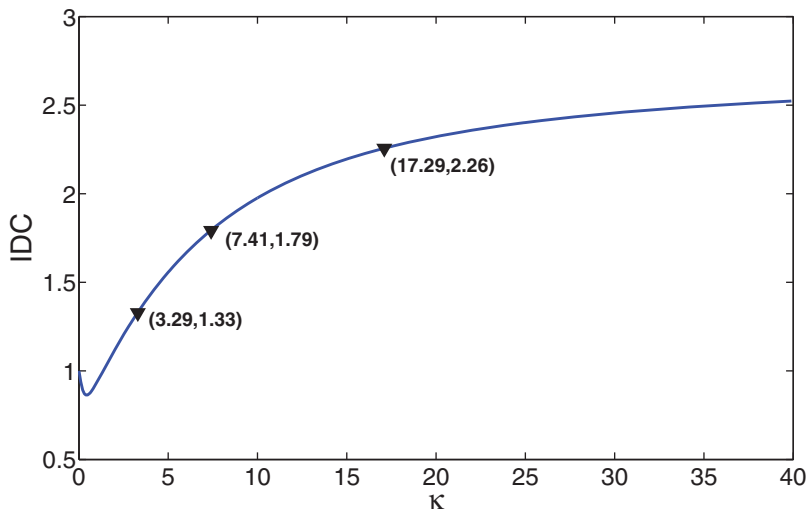


Figure 4. Example 2: IDC vs. κ .

Appendix 5: Number-in-system performance by case

Table 11. Fitting a MAP(2) to MAP(3), $\rho=.6$, via CIM, PM, DC, CED and EM.

Case	μ	Actual		CIM-APE _m		PM-APE _m		DC-APE _m		CED-APE _m		EM-APE _m	
		NS	CIM-NS	(%)	PM-NS	(%)	DC-NS	(%)	CED- NS	(%)	EM-NS	(%)	
1	3.6398	2.8068	2.7947	0.43	2.9236	4.16	4.2779	52.41	2.8068	0.00	3.0342	8.10	
2	3.6252	2.9237	2.9204	0.11	3.0613	4.71	5.6210	92.26	2.9237	0.00	2.9114	0.42	
3	3.6060	3.0622	3.0811	0.62	3.1140	1.69	5.1329	67.62	3.0620	0.01	3.0245	1.23	
4	3.5800	3.2279	3.0865	4.38	3.2172	0.33	3.2302	0.07	3.2273	0.02	3.2599	0.99	
5	3.5437	3.4282	3.3706	1.68	3.6622	6.83	3.4377	0.28	3.4262	0.06	3.4444	0.47	
6	3.4908	3.6714	3.5341	3.74	3.6574	0.38	3.6866	0.41	3.6660	0.15	3.5916	2.17	
7	3.4094	3.9627	3.9310	0.80	4.0728	2.78	3.9892	0.67	3.9495	0.33	4.1373	4.41	
8	3.2752	4.2860	4.2266	1.39	4.5000	4.99	4.3262	0.94	4.2545	0.74	3.9349	8.19	
9	3.0326	4.5105	4.4131	2.16	4.5541	0.97	4.5554	1.00	4.4429	1.50	4.1551	7.88	

Table 12. Fitting a MAP(2) to MAP(3), $\rho=.9$, via CIM, PM, DC, CED and EM.

Case	μ	Actual NS	CIM-NS	CIM-APE _m (%)	PM-NS	PM-APE _m (%)	DC-NS	DC-APE _m (%)	CED-NS	CED-APE _m (%)	EM-NS	EM-APE _m (%)
1	2.4265	16.8265	16.7558	0.42	17.3775	3.27	24.1026	43.24	16.8247	0.01	20.5548	22.16
2	2.4168	17.4504	17.4346	0.09	18.0775	3.59	28.9776	66.06	17.4498	0.00	17.3827	0.39
3	2.4040	18.1693	18.2763	0.59	18.3982	1.26	34.0968	87.66	18.1693	0.00	17.2582	5.01
4	2.3867	18.9958	18.2754	3.79	18.9257	0.37	19.0112	0.08	18.9951	0.00	18.6528	1.81
5	2.3625	19.9441	19.6427	1.51	21.4275	7.44	19.9900	0.23	19.9398	0.02	19.3327	3.07
6	2.3272	21.0189	20.3836	3.02	20.9546	0.31	21.0918	0.35	21.0048	0.07	20.5491	2.24
7	2.2730	22.1860	22.0354	0.68	22.7848	2.70	22.3067	0.54	22.1492	0.17	24.0111	8.23
8	2.1835	23.3347	23.1428	0.82	24.3522	4.36	23.5003	0.71	23.2491	0.37	21.9358	6.00
9	2.0217	23.9861	23.6666	1.33	24.2674	1.17	24.1631	0.74	23.8076	0.74	22.8815	4.61

Table 13. Fitting a MAP(2) to MAP(4), $\rho=.6$, via CIM, PM, DC, CED and EM.

Case	μ	Actual NS	CIM-NS	CIM-APE _m (%)	PM-NS	PM-APE _m (%)	DC-NS	DC-APE _m (%)	CED-NS	CED-APE _m (%)	EM-NS	EM-APE _m (%)
1	9.5238	1.4976	1.5582	4.05	1.6138	7.76	1.6121	7.65	1.6011	6.91	2.1139	41.15
2	9.5238	1.5069	1.5505	2.89	1.6146	7.14	1.6138	7.09	1.6165	7.27	1.7193	14.1
3	9.5238	1.5187	1.5781	3.91	1.6124	6.17	1.6159	6.40	1.6682	9.84	1.3329	12.23
4	9.5238	1.5339	1.5792	2.95	1.6130	5.16	1.6029	4.50	1.6406	6.96	1.7035	11.06
5	9.5238	1.5547	1.5948	2.58	1.5944	2.55	1.5990	2.85	1.5944	2.56	1.5171	2.42
6	9.5238	1.5846	1.6010	1.03	1.6158	1.97	1.6092	1.55	1.6158	1.97	1.6394	3.46
7	9.5238	1.6319	1.7170	5.21	1.6518	1.22	1.6301	0.11	1.6518	1.22	1.4863	8.92
8	9.5238	1.7191	1.7169	0.13	1.7284	0.54	1.6627	3.28	1.7292	0.59	1.5069	12.34

Table 14. Fitting a MAP(2) to MAP(4), $\rho = 0.9$, via CIM, PM, DC, CED and EM.

Case	μ	Actual NS	CIM-NS	CIM-APE _m (%)	PM-NS	PM-APE _m (%)	DC-NS	DC-APE _m (%)	CED-NS	CED-APE _m (%)	EM-NS	EM-APE _m (%)
1	6.3492	9.3283	9.7360	4.37	10.2107	9.46	9.9346	6.50	9.7629	4.66	16.4271	76.1
2	6.3492	9.4298	9.6522	2.36	10.2047	8.22	9.9586	5.61	9.8594	4.56	8.9846	4.72
3	6.3492	9.5600	9.8940	3.49	10.1688	6.37	9.9998	4.60	10.1576	6.25	5.3713	43.81
4	6.3492	9.7331	9.8780	1.49	10.3098	5.93	9.9884	2.62	10.0563	3.32	12.3618	27.01
5	6.3492	9.9743	9.9947	0.20	9.9888	0.15	10.0696	0.96	9.9889	0.15	9.2322	7.44
6	6.3492	10.3341	9.6174	6.94	10.3393	0.05	10.2246	1.06	10.3403	0.06	10.1031	2.24
7	6.3492	10.9286	10.3444	5.35	11.0990	1.56	10.6130	2.89	11.0992	1.56	7.9968	26.83
8	6.3492	12.0980	12.8672	6.36	14.1375	16.8	11.3819	5.92	14.1400	16.88	9.1537	24.34
9	6.3492	15.4028	14.6687	4.77	32.0882	108%	13.7196	10.93	53.7613	249.0	8.5055	44.78

Table 15. CIM-MAP(2) vs. CIM-MAP(3).

Case	$\rho=.6$					$\rho=.9$				
	Actual NS	MAP(2)-NIS-APE	MAP(2)-NIS-APE (%)	MAP(3)-NIS	MAP(3)-NIS-APE (%)	Actual NS	MAP(2)-NIS	MAP(2)-NIS-APE (%)	MAP(3)-NIS	MAP(3)-NIS-APE (%)
1	1.4976	1.5582	4.05	1.5524	3.66	9.3283	9.736	4.37	9.6501	3.45
2	1.5069	1.5505	2.89	1.5496	2.83	9.4298	9.6522	2.36	9.6308	2.13
3	1.5187	1.5781	3.91	1.5357	1.12	9.56	9.894	3.49	9.5956	0.37
4	1.5339	1.5792	2.95	1.5287	0.34	9.7331	9.878	1.49	9.6248	1.11
5	1.5547	1.5948	2.58	1.5506	0.26	9.9743	9.9947	0.20	9.8249	1.50
6	1.5846	1.601	1.03	1.6108	1.65	10.3341	9.6174	6.94	10.4048	0.68
7	1.6319	1.717	5.21	1.6635	1.94	10.9286	10.3444	5.35	10.9786	0.46
8	1.7191	1.7169	0.13	1.7727	3.12	12.098	12.8672	6.36	12.2967	1.64
9	1.9446	1.8579	4.46	2.0031	3.01	15.4028	14.6687	4.77	15.5407	0.90